Acoustic Cavitation. Experimental Results

Sergei Peshkovsky

Ultrasound Sources for Producing Cavitation

Introduction

It is well known that ultrasonic transducers are incapable of creating vibrations with sufficiently large amplitudes to produce a well-developed cavitation area. Acoustic horns, which look like tapering resonant sonotrods, are commonly used in order to alleviate this problem. They are capable of magnification of the ultrasonic amplitude along with reduction of the radiation output surface. Such horns can not provide a large output surface and a high gain simultaneously. Therefore, they do not permit transmission of all available acoustic energy from the transducer into liquid.

Acoustic Radiators for Industrial Sonochemistry

Acoustic radiators with large radiating surfaces are necessary for the realization of sonochemical processes on an industrial scale. Application of powerful magnetostrictive transducers as acoustic converters seems to be the best solution for industry.

The specific mechanical power, which a magnetostrictive transducer can transfer to the load, is limited by two factors: the ultimate magnetostrictive oscillatory stress of saturation $\boldsymbol{\tau'_t}$ and the limiting oscillatory velocity $\mathbf{V'_t}$ determined by the fatigue strength. (All primed symbols here and below are peak to peak values; all non primed - are root-mean-square values.)

(1) $\boldsymbol{\tau'_t = e'E\,\psi_1}$,

(2) $\mathbf{V'_t = \sigma'\psi_2 / \rho_t C_t}$.

Where: $\mathbf{e'}$- is the ultimate magnetostrictive strain of saturation; $\mathbf{E}$ – is the modulus of elasticity (Young's modulus); $\boldsymbol{\sigma'}$ - is the fatigue strength; $\boldsymbol{\psi 1}$ and $\boldsymbol{\psi 2}$ - are the shape factors of the transducer; $\boldsymbol{\rho_t}$ and $\mathbf{C_t}$ – are the density and the thin-wire sound wave speed of the transducer material respectively.

Let us assume that the transducer is already transferring the maximum power to the load with the help of the horn. Then, the following relationship should hold:

(3) $\boldsymbol{\tau'_t / V'_t = rK^2 N^2}$,

or

(4) $\boldsymbol{\tau'_t / rV'_h = KN^2}$.

Where: $\mathbf{r}$ – is the active component of the load acoustic resistance; $\mathbf{V'_h}$ **–** is the output oscillatory velocity; $\mathbf{V'_t}$ **-** is the input oscillatory velocity; $\mathbf{K = V'_h / V'_t}$ – is the gain factor of the acoustic horn; $\mathbf{N = D_h / D_t}$**;** $\mathbf{D_h}$ **–** is the diameter of the horn's output section; $\mathbf{D_t}$ **-** is the diameter of the horn's input section (transducer output section.) See Fig.1.

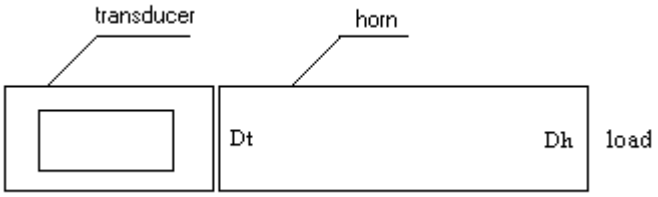

Fig. 1. Ttransducer with matching horn.

The factor of a travelling wave can be calculated as follows:

(5) $\mathbf{k_t = rK^2N^2/\rho_tC_t}$,

or

(6) $\mathbf{k_t = e'E\psi_1 / \sigma'\psi_2}$.

Substituting in Eq. (1) the properties of basic magnetostrictive materials makes it clear that the mode of a standing wave is kept even for the matched transducer, as $\mathbf{k_t} << 1$. Thereby, applying the well-known methods and using the reactive component of the acoustic load's resistance we can carry out the design of the resonance dimensions of the discussed horns. It is important to notice that the reactive component of the acoustic load's resistance is equal to zero for liquids at cavitation.

Let's further consider the problem of matching the transducer only with an active component of the load resistance, for example the matching of a magnetostrictive transducer to water at cavitation.

According to experimental results the radiation energy intensity **E** dissipated in water at cavitation can be approximately equated with Eq. (7). See Eq. (12) and Fig.(11.)

(7) $\mathbf{E/P_0 \approx (V_h - V_0).}$

Where: $\mathbf{P_0}$ **–** is the static pressure; $\mathbf{V_0 = P_0/\rho C}$; $\boldsymbol{\rho}$ **–** is the density of water; **C** – is the sound wave speed in water.

It is reasonable to make an approximation based on Eq. (7) that the complete energy intensity radiating by a transducer into the load is equal to:

(8) $\mathbf{I = E + I_0 = P_0V_h}$.

Where: $\mathbf{I_0 = P_0V_0}$ **–** is the energy intensity outside the cavitation area.

The recoil reaction of the load to the horn (acoustic pressure) is approximately equal to $\mathbf{P_0}$:

(9) $\mathbf{Po \approx 0.7rV'_h,}$

and

(10) $\mathbf{\tau'_t / rV'_h \approx 0.7e'E\psi_1 / P_0.}$

Hence, a matched transducer must be supplied with the horn that has the following combination of parameters **K** and **N**:

(11) $\mathbf{KN^2 \approx 0.7e'E\psi_1 / P_0.}$

The values of $\mathbf{KN^2}$ at $\mathbf{P_0}$ = 1 bar and $\mathbf{\psi_1}$ = 0.45 for the basic magnetostrictive materials are the following: Alfer – 17.4; Permendura – 44.5; Nickel – 22.8; Ferrite – 15.6. (According to data in Ref. [1].)

It is also possible to match an industrial transducer to water at cavitation according to its nominal acoustic power value.

Acoustic horns, which look like tapering (or hollow widen) resonant sonotrods, can not provide a large output surface and a high gain simultaneously. Therefore, they do not permit transmission of all available acoustic energy from the transducer into water at cavitation. We have designed a series of powerful acoustic horns capable of providing large output surfaces simultaneously with high gain, which call - "barbell horn". These devices can accurately match a transducer to water at cavitation, thereby permitting the transmission of all available acoustic potential energy.

A barbell horn for a magnetostrictive transducer and a ceramic transducer with the barbell horn are shown in Fig. 2.

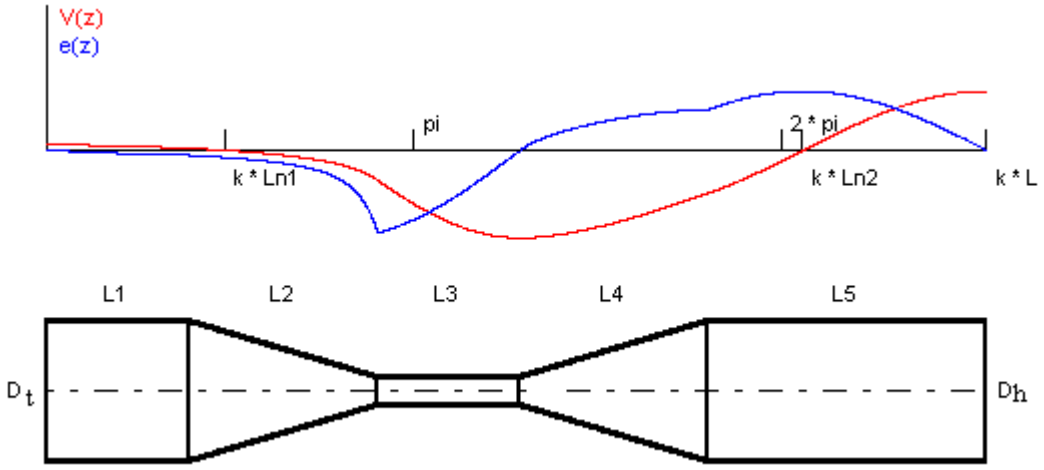

a

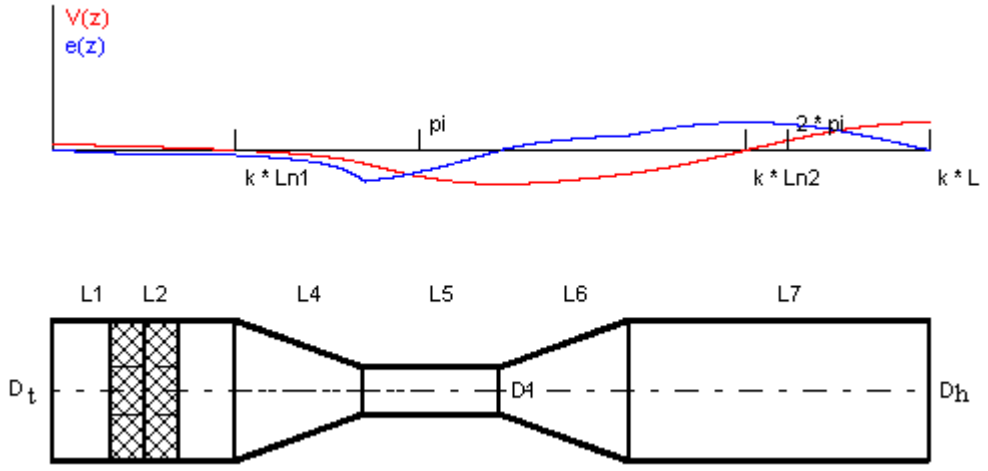

b

Fig. 2. Barbell horn (a) and ceramic transducer with barbell horn (b).
(**V(z)** – current oscillatory velocity, **e(z)** - current oscillatory strain, **k** - wave number, **Ln1** and **Ln2** - nodal points, **L** - general length)

We have also designed another type of acoustic horns, called "barrel horns", that can match a transducer to water at cavitation. See Fig. 3.

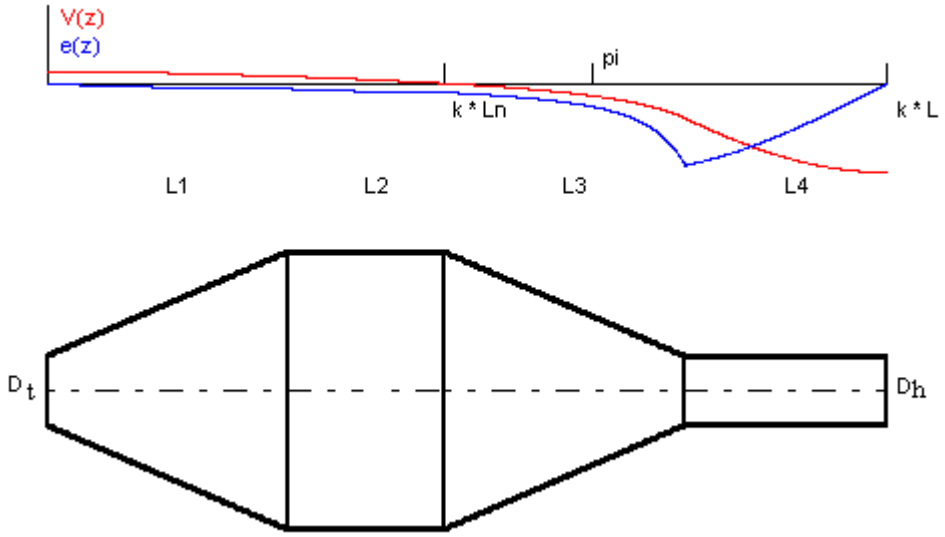

Fig. 3. Barrel horn.
(**V(z)** – current oscillatory velocity, **e(z)** - current oscillatory strain, **k** - wave number, **Ln** - nodal point, **L** - general length)

However, even barbell and barrel horns are not always capable of supplying the required radiating surfaces and the dwelling time of the working liquids in the ultrasonic reactor. The design of special acoustic systems, based on barbell horns, that are capable of providing extra large radiation surfaces, is a real necessity for many industrial applications.

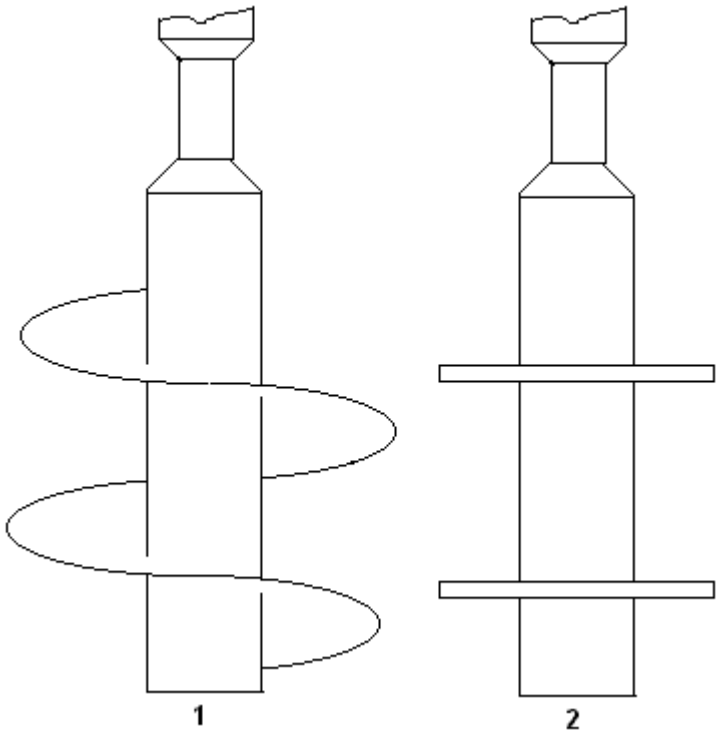

Fig. 4. Acoustic systems with extra large radiating surfaces.

System **1** has a continuous radiating surface, winded around the barbell horn. System **2** has a discrete radiating surface, i.e. resonant round plates connected to the barbell horn.

Fig. 5. Photograph of a real acoustic system 1.

It is also possible to design an acoustic system based on a resonant hollow sphere and a round magnetostrictive transducer. See Fig. 6.

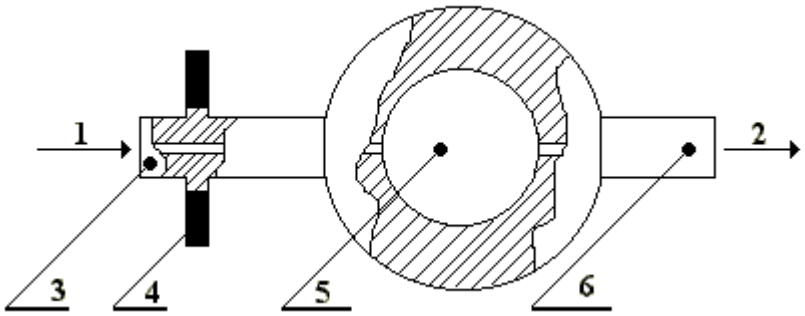

Fig.6. Acoustic system with a resonant hollow sphere. (1 – intake of liquid, 2 – output of liquid, 3, - barbell horn, 4 – annular magnetostrictive transducer, 5 - resonant sphere, 6 – acoustic sonotrod.)

In the system shown in Fig.6 radial oscillations of the annular transducer are transformed into axial oscillations form and magnify with the help of the barbell horn, and then are converted into radial oscillations of the resonant sphere. Working liquid comes into the sphere from the input 1 and leaves sphere from the output 2. Amplitude of oscillations can reach very high values in the center of the oscillating sphere.

We have also developed computer-aided design of a number of types of circular multi-echelon horns (hollow horns, step horns with exponential, catenoidal and conical transitional echelon, as well as barbell and barrel horns) with low stresses at the steps and, therefore, with long lifetimes (longevity).

Experimental Examination of Water at Cavitation

Introduction

The propensity to cavitation is inherent in all low-viscous fluids without exception because of their inability to withstand tensile stresses. It is one of the fundamental properties of the liquid state of a substance. The cavitation area exhibits uncommon “technological activity”. It is capable to emulsify fluids, destroy surfaces of rigid bodies, accelerate chemical reactions, etc. This essentially creates a significant application value of the phenomenon. It would be reasonable to assume that technological activities are being shaped inside the boundaries of the cavitation area, and hence, are determined by the collective behavior of cavitation bubbles included in the accumulation (“assembly”).

Experimental Results

A number of experimental methods of examination of acoustic cavitation have been disclosed in technical and scientific literature. The overwhelming majority are based on

indirect studies of the secondary effects of cavitation, such as disintegration of rigid samples located in the cavitation area, acceleration or initiation of chemical reactions, dispersion of solid particles, emulsification of fluids, etc. Methods of direct measurements of cavitation performance have also been applied using different sound probes, thermocouples, etc.

The most acceptable is a group of experimental methods based on a measurement of the energy on the electrical side of a transducer, or on direct measurement of the radiation energy absorbed in the cavitation area using calorimetric methods. Such examinations reveal the dependence of the emitted energy intensity from the oscillatory velocity of the acoustic transducer (or horn) without disturbing and changing the actual structure of the cavitation area.

The following experimental data [2] were obtained by measuring the radiation energy intensity on electrical side of a transducer operated in the water before and during cavitation. See Fig.7.

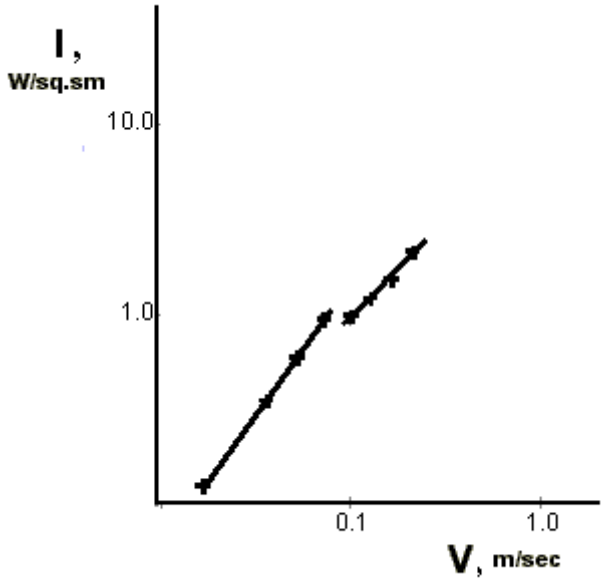

Fig.7. Radiation energy intensity I as a function of oscillatory velocity V.

It can be seen in Fig.7 that a "jump" occurs in the acoustic properties of water when the oscillatory velocity **V** reaches approximately the value of $\mathbf{V_0}$ ~ 0.1m/sec. Hence, $\mathbf{V_0}$ exhibits the threshold of acoustic cavitation.

The real-time measurements of the acoustic energy intensity dissipated in water in the range of the oscillatory velocities from 0.25 m/sec to 12 m/sec were carried out by using a water calorimeter. The frequency of the acoustic transducer was 17.8 kHz. The required values for the oscillatory velocity **V** were achieved by using a replaceable set of barbell horns with varying gain factors and a constant output surface.

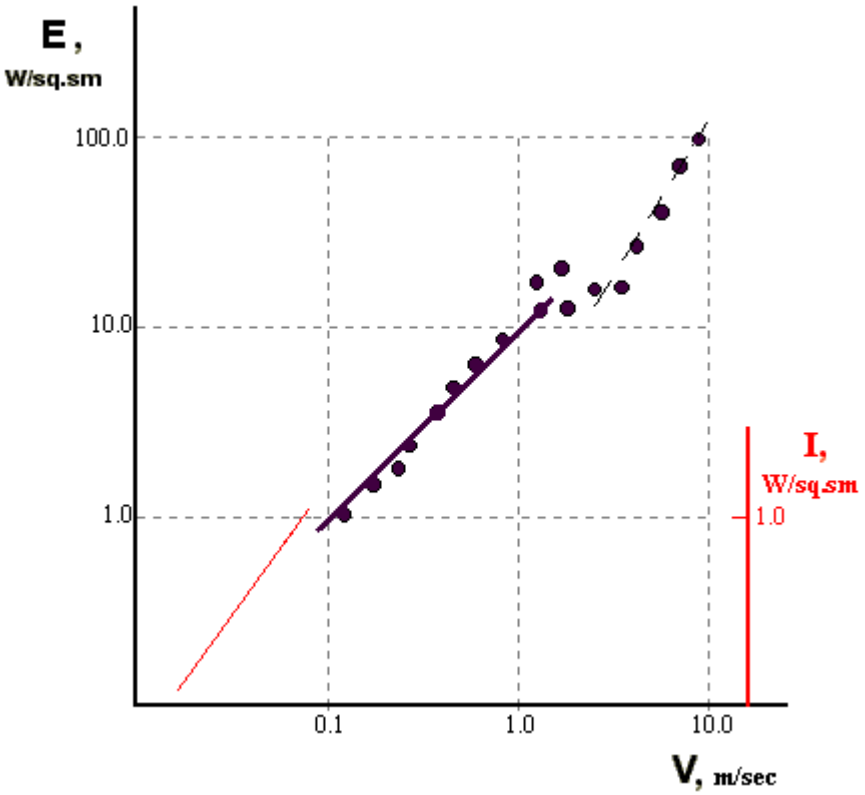

Fig.8. Radiation energy intensity E dissipated in cavitation area as a function of oscillatory velocity V.

In Fig.8 the red line illustrate the radiation energy intensity in linear area of radiation without cavitation, when $\mathbf{I \sim V^2}$**.** It is important to emphasize that the phenomenon called "the second threshold of acoustic cavitation" has been revealed at the oscillatory velocity in the narrow range from 3 m/sec to 5 m/sec. The exact value of this threshold parameter depends on the particular procedure of water preparation for the experiments.

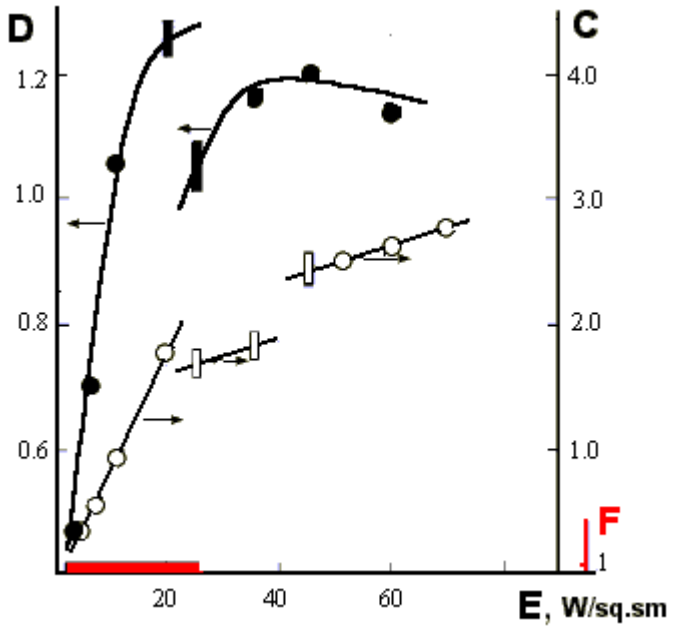

Fig.9. Test measurements of the cavitation area activity.
(**D** – character of dispersion, **C** – character of sonochemistry,
F – character of erosion)

Various secondary effects accompanying acoustic cavitation were also investigated. Typical results of the experiments are shown in Fig.9. Coordinate **D** characterizes the dispersion of graphite particles with an average size of 200 μ. The particle dispersion has been characterized after the acoustic cavitation treatment by using a photocolorimeter. The parameter **C** on the right axis of the same graph describes the uprise of free iodine from a solution of potassium iodine in water at acoustic cavitation, and coordinate **F** estimates the erosion of aluminum foil after the same cavitation treatment.

Changes in the graph's shape and the breaks of the curves are exhibited in Fig.9 where **E** > 30 W/sq.sm. Destruction of aluminum foil also stopped. It is possible to conclude that after the point, where **E** > 30 W/sq.sm, acoustic cavitation passes into another stage – acoustic supercavitation, analogous to a hydrodynamic form of cavitation.

The water calorimeter made it possible to carry out the experiments at varying values of static pressure $\mathbf{P_0}$. The pressure was created by compressed nitrogen. Typical results of these experiments are shown in Fig.10.

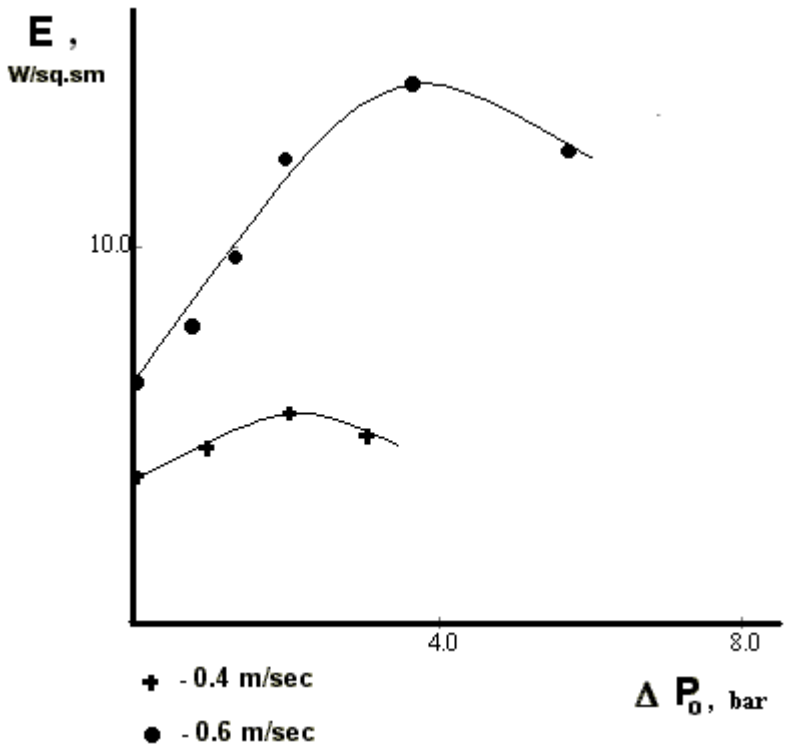

Fig.10. Radiation energy intensity E dissipated in the cavitation area as a function of static pressure ΔP_0.

All the results of the measurements of the radiation energy dissipated in the cavitation area are shown in Fig.11 in a consolidated form, invariant with respect to $\mathbf{P_0}$.

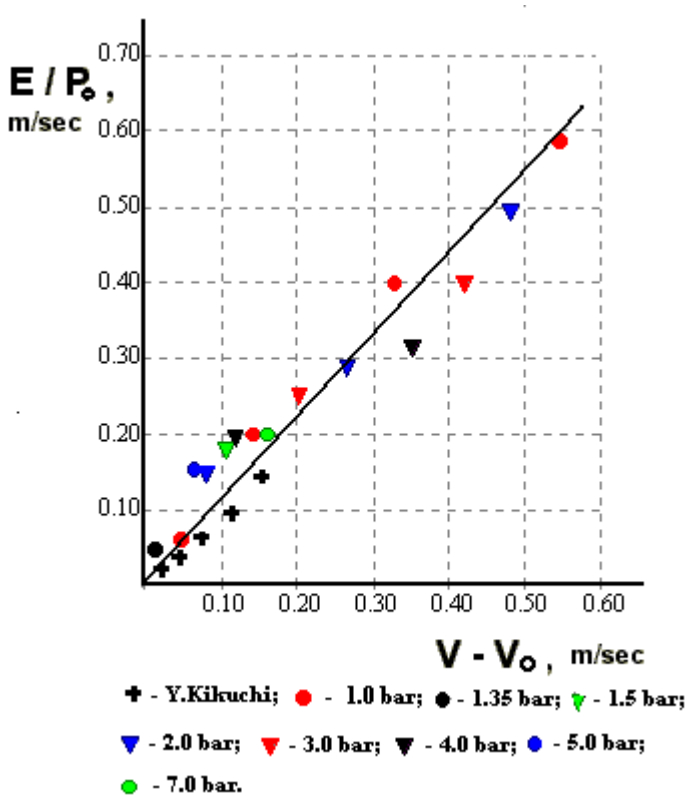

Fig.11. Radiation energy intensity E dissipated in the cavitation area as a function of oscillatory velocity V. (P_0 **-** static pressure; $V_0 = P_0/\rho C$ **-** parameter of normalization, **ρ -** density of water, **C** - sound wave velocity in water)

The results in Fig.11 can be approximated with the following expression:

(12) $\mathbf{E/P_0 = 1.1(V - V_0).}$

It is easy to show that **E** reaches maximum value, when $\mathbf{P_0 \approx 0.5\rho C.}$

Author has made an attempt to develop a physical model of the cavitation area based on known representations of dynamics of compressible liquid. The set of equations obtained on the basis of these representations has finite solutions and it is possible with their help to calculate many energy parameters of the cavitation area. The phenomenon of the first and the second thresholds of cavitation can be explained within the framework of the proposed model.

Experimental Examination of Molten Polymers at Cavitation

Introduction

It has been shown in the past that for molten polymers, strained under the condition of the triaxial stress state, static tensile stresses, at which cohesive destruction takes place, do not exceed 1 MPa,. This corresponds to the static strength value for low-viscous fluids. Consequently, acoustic cavitation can also be expected in molten polymers under certain conditions at a relatively low intensity of acoustic treatment. High-viscous polymer systems characterized by viscous elasticity or, in other words, demonstrating the properties both of liquid and of elastic bodies simultaneously were the subjects of our further experiments.

Experimental Results

To identify and evaluate the threshold of acoustic cavitation in high polymers a special set-up was used..

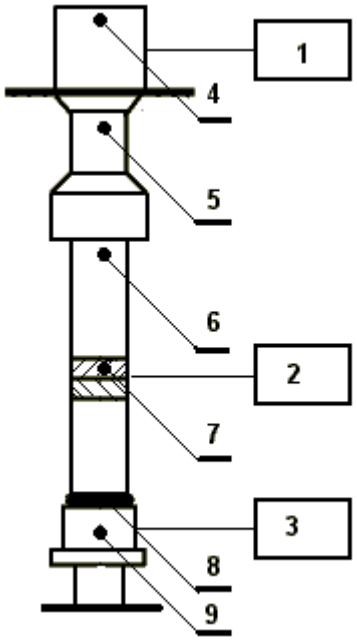

Fig. 12. The experimental set-up for evaluating the threshold of acoustic cavitation in high polymers.
(1 – ultrasonic generator, 2,3 – recording devices, 4 – magnetostrictive transducer, 5, – barbell horn, 6 – sonotrod, 7,9 - ceramic receivers, 8 – polymer sample.)

The ultrasonic generator stimulated acoustic oscillations at a frequency of 17.8 kHz. With the help of the barbell horn, these oscillations were transferred to the high polymer, situated in the gap between the horn and the ceramic receiver. The thickness of the gap was 1 mm. The ceramic receiver 2 controlled the amplitude of the input oscillations. The ceramic receiver 3 controlled the amplitude of the output oscillations. Samples of polybutadiene of narrow MWD and Newtonial viscosity about of 10^5 - 10^6 Pa * sec were used for measurements. The tests were carried out at the room temperature.

At the amplitude of the horn insufficient for cavitation recorded by receivers 2 and 3 data are rather close, since the acoustic energy losses in subcavitating liquid are small. With an

increase in amplitude, the acoustic oscillations recorded at the receivers also increase. While passing the cavitation threshold, the critical amplitude of oscillation **A** at the receiver 3 remains stable and becomes independent of the amplitude of horn oscillations, as a result of the strong dissipation of the supplied acoustic energy in the cavitation area formed in the polymer.

The experimental results are given in Fig.13.

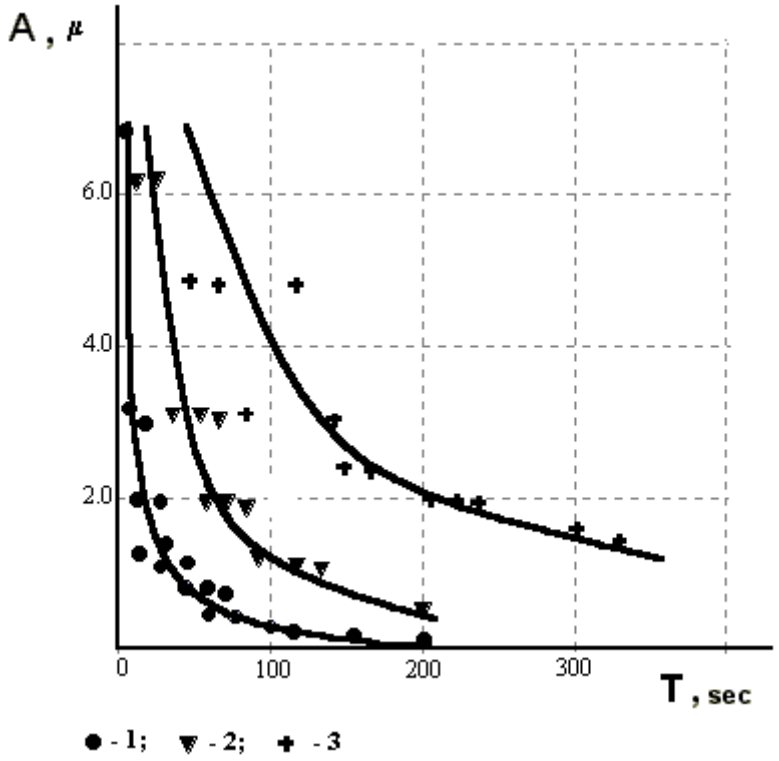

Fig. 13.The threshold amplitude of acoustic oscillations A as a function of time of treatment T.

(M – molecular weight, 1 – M = 1.6 * 10^5; 2 – M = 3.5 * 10^5; 3 – M = 5.3 * 10^5.)

It is clear that for cavitation the critical amplitude of acoustic oscillations **A** is time-depended, i.e. it is characterized by the long-term strength typical for high polymers. The stability of high polymers, with respect to the cavitation formation, increases with molecular weight. At rather large amplitudes, these dependencies can be satisfactory described by an exponential function while, at low amplitudes, they obey a power law.

The fact that the critical amplitude **A** is a function of acoustic treatment time appears to be connected with the growth of cavitation nuclei. Under the action of the acoustic field, these nuclei gradually increase dimensions, which are determined by the diffusion conditions. Similar phenomenon has been theoretically shown in water. However, the times necessary for establishing the equilibrium cavitation radii in low-viscosity liquids are only several acoustic oscillations and, therefore, are not usually registered.

The set-up shown in Fig.14 was used for visualizing processes occurring under the action of the acoustic field in high polymers.

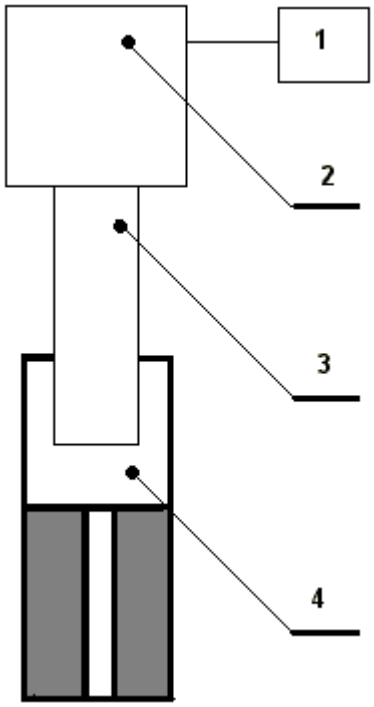

Fig. 14. The experimental set-up for studying the effects of the cavitation area in polymers.
(1 – ultrasonic generator, 2 – magnetostrictive transducer, 3 – ultrasonic barbell horn, 4- transparent walls of the chamber and slotted capillary.)

The frequency of the acoustic transducer was 17.8 kHz. The barbell horn was fixed in a chamber filled with the test material. A slotted capillary (30-10-3.2 mm) was placed in the lower part of the chamber. The capillary and the chamber had transparent walls. Polymer was supplied to the chamber trough an inlet with the help of compressed nitrogen. The transparent walls of the chamber allowed observation of the processes occurring during the treatment of flowing polymer with ultrasound.

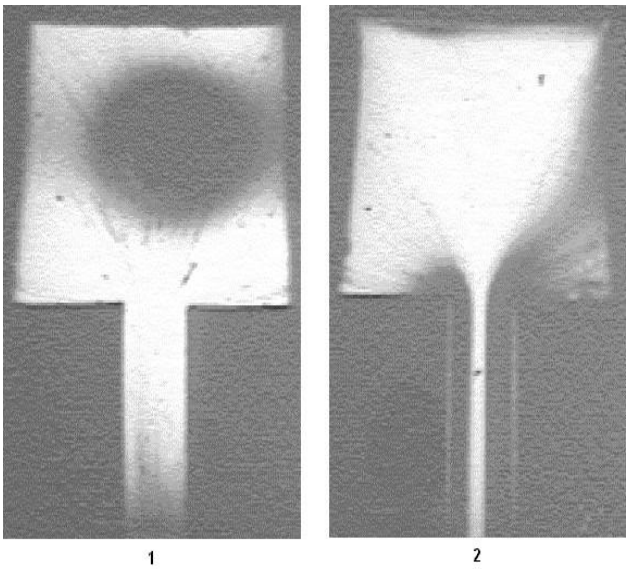

Fig. 15. 1 - growth of cavitation bubbles around the source of cavitation nuclei in the acoustic field; 2 – the cavitation area in the flowing polymer.

Bubbles form near the oscillator and the walls of the chamber and the capillary. Their formation can also be induced near the source of cavitation nuclei introduced into polymer. In Fig.15–1 the growth of the cavitation area is shown. The cavitation area, formed in flowing polymer by the acoustic field, is shown in Fig.15–2. Of the special interest here is the distribution of bubbles in the slotted capillary. The zone adjoining the axis of the flat – slotted channel does not contain bubbles. Here, the largest hoop stresses are observed. Moreover, bubbles are not formed in the boundary layers, where maximum shear stresses occur.

The acoustic treatment of molten polymers may be very successful. Major methods of thermoplastic processing are based on their transition to the viscoflowing state and, therefore, the possibility of obtaining free radicals in molten polymer at acoustic cavitation opens a way for mechanical and chemical transformation of thermoplastics directly at the stage of their processing into products. Compared to the known methods of mechanochemical destruction of macromolecules in molten polymers (screw plastication, etc) the acoustic cavitation offers wider opportunities to control the depth of the processes. An important point is that standard processing equipment can be easily equipped with the acoustic treatment systems.

Acknowledgements

The author would like to thank A. Iakovlev, M. Friedman, V. Monachov and A.Tukachinsky for participation in the work.

References

[1] E.A. Neppiras. Acoustica, 1968, 19, 1, p.54.
[2] K. Fukushima, J. Saneyoshi, Y. Kikuchi, in Y. Kikuchi (Ed.). Ultrasonic Transducers, Corona Publ. Co., LTD, Tokyo, 1969.